

Computer Simulation of Fundamental Behaviors of Point Defects, Clusters and Interaction with Dislocations in Fe and Ni

E. Kuramoto, K. Ohsawa and T. Tsutsumi¹

Abstract: In order to investigate the interaction of point defects with a dislocation, an interstitial cluster or a SFT (stacking fault tetrahedron), computer simulation has been carried out in model Fe and Ni crystals. The capture zone (the region where the interaction energy is larger than kT) was determined for various interactions. Calculated capture zone for $T = 500^\circ\text{C}$ for SIAs (crowdion and dumbbell) around a straight edge dislocation is larger than that for a vacancy in both Fe and Ni. Capture zones for Ni are larger than those for Fe, suggesting that Ni (fcc) has a larger dislocation bias factor than Fe (bcc). Capture zone calculated for an interstitial cluster (dislocation loop) I_{61} is smaller than that for a straight edge dislocation, especially in Fe. Capture zones were also calculated for an SFT V_{28} in Ni, indicating a larger capture zone with SIAs (crowdion and dumbbell) and a smaller capture zone with a vacancy.

keyword: SIA(self-interstitial atom), vacancy, dislocation, dislocation loop, SFT (stacking fault tetrahedron), bias factor, iron, nickel, computer simulation

1 Introduction

In the development of materials used under irradiation environments like fusion and fission reactors it is very important to clarify the fundamental mechanism of the evolution of the damage structure. For this purpose the so-called bias mechanism is the most important event. The important bias mechanisms that have so far been presented include: i) dislocation bias [1] and ii) production bias [2-4]. In the former the interaction between a straight edge dislocation and freely migrating defects plays a central role. Usually self-interstitial atoms (SIAs) interact with an edge dislocation stronger than vacancies. This preference results in the accumulation of excess vacancies in the matrix, which is the basic driving force

for void nucleation and growth. This is the fundamental mechanism of the dislocation bias. On the other hand, in the latter the cascade production event itself is responsible for the bias mechanism. Namely it is recently recognized by large scale computer simulations that interstitial clusters are already produced during cascade formation process and these clusters are usually bundles of crowdions ($\langle 111 \rangle$ crowdions for bcc metals, $\langle 110 \rangle$ crowdions for fcc metals) and very mobile one-dimensionally [3,4]. They easily migrate one dimensionally to sinks like dislocations and grain boundaries. This again contributes to the accumulation of excess vacancies in the matrix, resulting in the void nucleation and growth.

In the interactions described here detailed studies of the elementary processes are required, such as the interaction between an edge dislocation and point defects, atomic structures of clusters of SIAs, dynamic behaviors of clusters of SIAs, the interaction between an SFT (stacking fault tetrahedron) and point defects, and the interaction between a moving dislocation and various kinds of defects.

In this paper the interaction between an edge dislocation and point defects, that between an interstitial cluster (dislocation loop) and point defects, and that between an SFT and point defects in Fe and Ni will be studied using computer simulations.

2 Computational Method

Model crystals of Fe and Ni were constructed by using EAM type potentials, that is, Finnis-Sinclair potential for Fe [5] and that developed by Gao, Bacon and Ackland for Ni [6]. Size of the model crystals must be large enough because defects usually have strain fields around them, especially, a dislocation has a long range strain field around it. Typical sizes of the model crystals are $80b \times 80(2 \cdot 2^{1/2}/3)b \times 80(2/3)^{1/2}b$ and $80b \times 80(3^{1/2}/2)b \times 80(2/3)^{1/2}b$ (b : the magnitude of Burgers vector) for Fe and Ni, respectively as shown in Fig.

¹ Research Institute for Applied Mechanics, Kyushu University
6-1 Kasuga-koen, Kasuga-shi, Fukuoka 816-8580

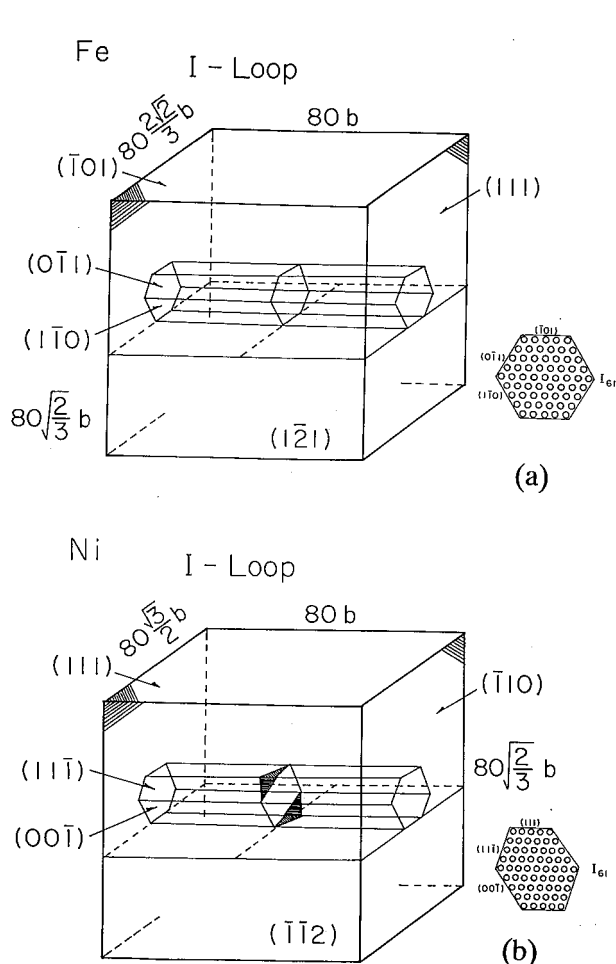


Figure 1 : Fe and Ni model crystals of sizes of $80b \times 80(2 \cdot 2^{1/2}/3)b \times 80(2/3)^{1/2}1/2b$ and $80b \times 80(3^{1/2}/2)b \times 80(2/3)^{1/2}b$, respectively. Interstitial clusters (dislocation loops) are constructed in the central parts of the model crystals.

1. This size is large enough to remove the size dependence of the result, which was confirmed by the calculation performed changing the size of the model crystals. Dislocations, clusters of self-interstitial atoms (SIAs) and stacking fault tetrahedra are introduced into the central part of the model crystals and the whole crystal was fully relaxed by the static method under the fixed boundary condition [7-9]. The behavior of the interaction between these defects and point defects must be extensively studied in order to obtain the information on the bias factor which is definitely important in the evolution of the damage structure during irradiation.

Fe
Interaction between an Edge Dislocation and a Crowdion (type A)

(Contour of -0.067 eV (500°C))

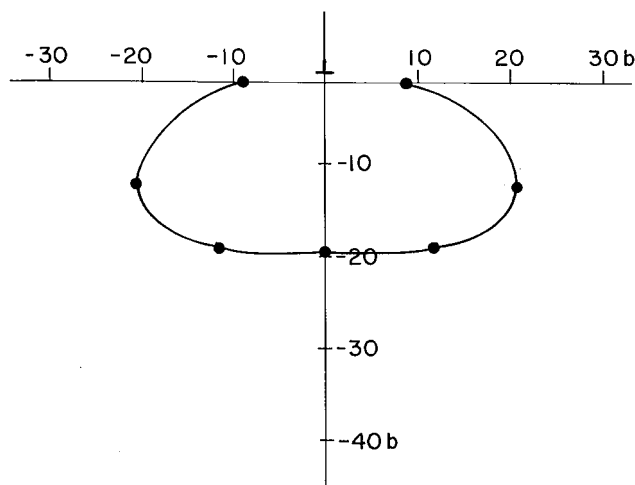


Figure 2 : The calculated capture zone for a crowdion around a straight edge dislocation in Fe (the axis of a crowdion is parallel to the Burgers vector of the edge dislocation).

3 Results and Discussion

3.1 Interaction between an edge dislocation and point defects

Both in Fe and Ni model crystals it is observed that an edge dislocation has an attractive strain field for an SIA in the tensile side, and for a vacancy in the compressive side. Defining a capture zone as the region where the interaction energy is larger than kT , we calculated capture zones for $T = 500^\circ\text{C}$ for various cases in order to obtain the information on the dislocation bias factor.

In Figs. 2 and 3 calculated capture zones for a crowdion around a straight edge dislocation in Fe, where the axis of a crowdion is parallel to the Burgers vector of the edge dislocation, and that for a vacancy in Fe are shown, respectively. In Fig. 4 the capture zone is also calculated for a crowdion around a straight extended edge dislocation (two partial dislocations and stacking fault region between them) in Ni (the axis of a crowdion is parallel to the total Burgers vector of the extended edge dislo-

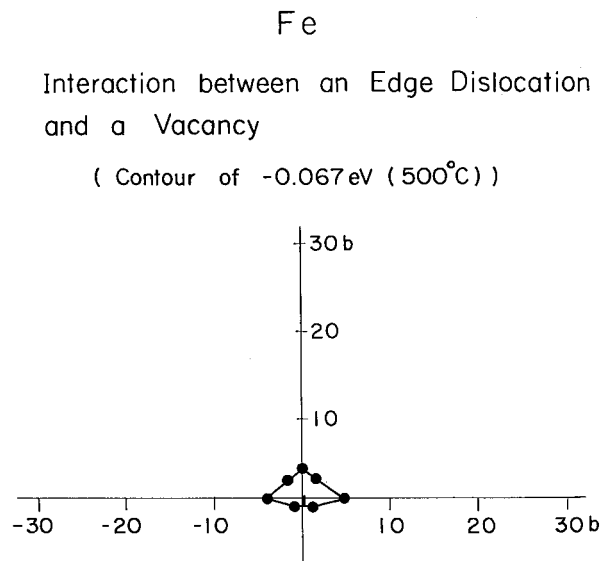


Figure 3 : The calculated capture zone for a vacancy around a straight edge dislocation in Fe.

cation). It was found that a straight edge dislocation has much larger capture zone for an SIA than for a vacancy in both Fe and Ni, although the absolute value of the capture zone depends on the type of an SIA (crowdion or dumbbell) and the orientation of an SIA to the Burgers vector of an edge dislocation. In Fig. 5 the comparisons of the calculated zone area for various cases, that is, a straight edge dislocation and crowdions of two orientations (A and B) and dumbbells of two orientations (A and B) and a vacancy in Fe and Ni are shown. A is parallel or near parallel to the Burgers vector of the edge dislocation, and B is perpendicular or near perpendicular to the Burgers vector. It is found that the capture zone for an SIA in Ni is much larger than that in Fe, suggesting that fcc metals have larger dislocation bias factor than bcc metals. This result is considered to be due to the difference of the relaxation volume of an SIA in Fe and Ni, namely, the former is smaller than the latter as discussed in the literature [10]. The size of the capture zone plays an important role in determining the bias factor, but the absorbability of point defects into the dislocation core is also the important factor. Within the capture zone the formation energy of point defects decrease, namely, the binding energy increases along the path towards the dislocation core and defects are finally absorbed into the core, especially in the vicinity of the dislocation core defects are spontaneously absorbed into the core as discussed in the litera-

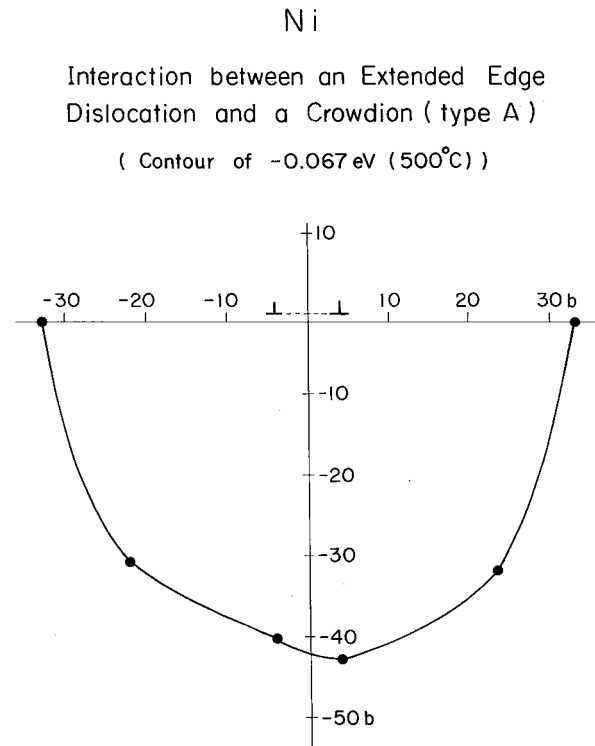


Figure 4 : The calculated capture zone for a crowdion around a straight extended edge dislocation (two partial dislocations and stacking fault region between them) in Ni. The axis of a crowdion is parallel to the total Burgers vector of the extended edge dislocation.

ture [11]. More detailed research will be needed for this absorption behavior of point defects into the dislocation core or the jogs on the dislocation line including alloy system. In alloy system, e.g., in V-Fe system the very interesting effect was observed in computer simulation, that is, a V-Fe mixed dumbbell has higher absorbability into the dislocation core than a crowdion [12].

3.2 Interaction between interstitial clusters (dislocation loops) and point defects

Capture zones for SIAs and a vacancy were also obtained for interstitial clusters (dislocation loops) in both Fe and Ni. Results for the interaction between I_{61} (bundle of 61 crowdions with the Burgers vector being $a/2 \langle 111 \rangle$) and a crowdion with the axis parallel to the Burgers vector, and that between I_{61} and a vacancy in Fe are shown in Figs. 6 and 7, respectively. From the comparison between the result for a straight edge dislocation and that for an interstitial cluster (bundle of crowdions) it is found

Interaction between an Edge Dislocation and SIA, V

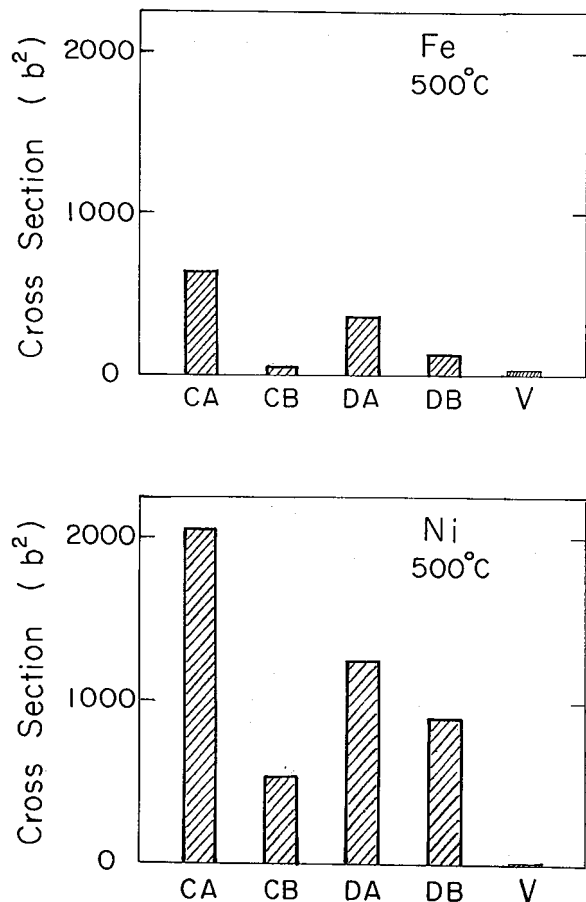


Figure 5 : Comparison of the calculated zone area for various cases, that is, a straight edge dislocation and crowdions of two orientations (A and B) and dumbbells of two orientations (A and B) and a vacancy in Fe and Ni. A is parallel or near parallel to the Burgers vector of the edge dislocation, and B is perpendicular or near perpendicular to the Burgers vector.

Fe

Interaction between I-Loop (I_{61}) and a Crowdion (type A)

(Contour of -0.067 eV (500°C))

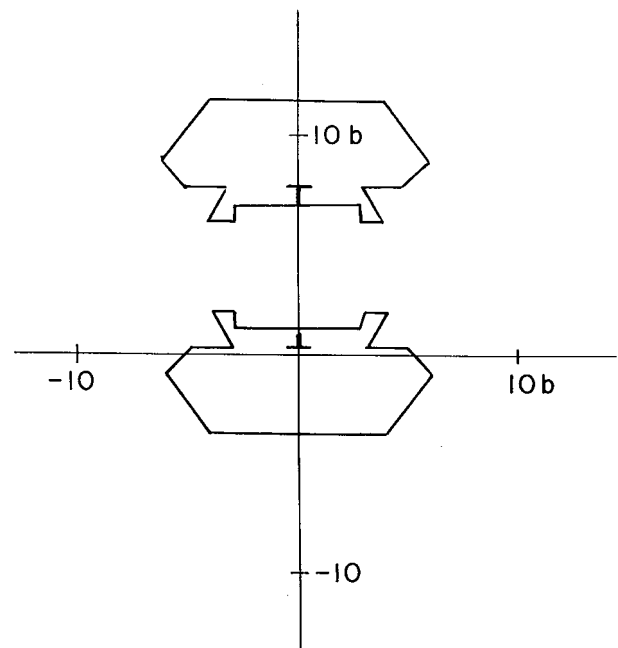


Figure 6 : The calculated capture zone for a crowdion around an interstitial cluster I_{61} (bundle of 61 crowdions with Burgers vector being $a/2\langle 111 \rangle$) in Fe. The axis of a crowdion is parallel to the Burgers vector of the interstitial cluster I_{61} , dislocation loop.

Fe

Interaction between I-Loop (I_{61}) and
a Vacancy
(Contour of -0.067 eV (500°C))

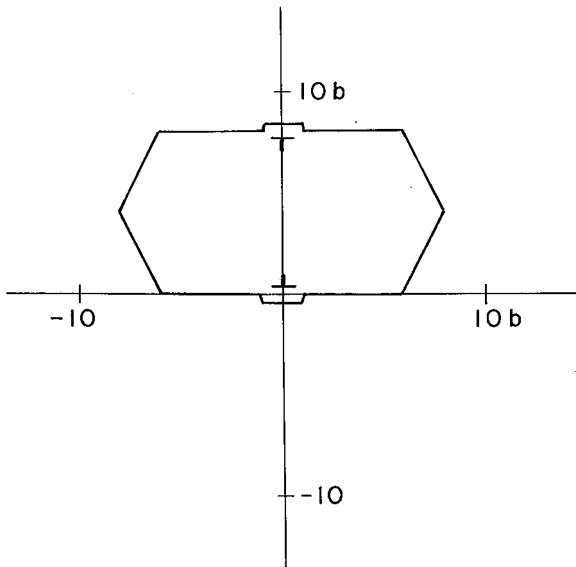


Figure 7 : The calculated capture zone for a vacancy around an interstitial cluster I_{61} (bundle of 61 crowdions with Burgers vector being $a/2\langle 111 \rangle$) in Fe.

that capture zone of an SIA (crowdion) for I_{61} in Fe is much smaller than that for a straight edge dislocation, of the order of about 20%. This is considered to be due to the overlapping and weakening of the two strain fields of the two edge dislocation segments of the opposite sign of the loop. On the other hand, the capture zone of a vacancy for I_{61} in Fe is larger than that for a straight edge dislocation. This result cannot be expected from the above discussion for a crowdion on the standpoint of the strength of the strain field. This is considered to be due to the fact that the recombination between a vacancy and a crowdion in I_{61} which lies on the same $\langle 111 \rangle$ atomic row as the vacancy occurs during lattice relaxation. This recombination is not observed in the interaction between a vacancy and a straight edge dislocation, but observed in that between a vacancy and interstitial clusters (dislo-

Ni

Interaction between I-Loop (I_{61}) and
a Crowdion (type A)
(Contour of -0.067 eV (500°C))

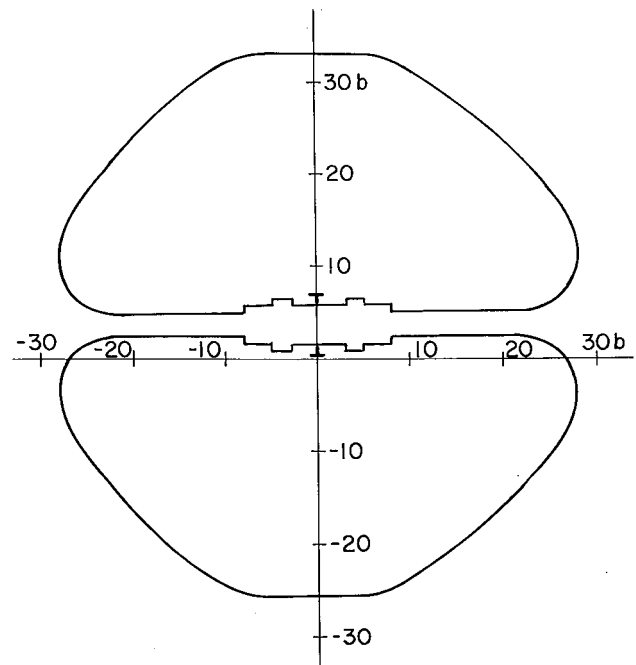


Figure 8 : The calculated capture zone for a crowdion around an interstitial cluster I_{61} (bundle of 61 crowdions with Burgers vector being $a/2\langle 110 \rangle$) in Ni.

cation loops), which was described in the previous paper [7]. These results suggest that an interstitial cluster has a smaller bias factor than a straight edge dislocation in Fe. In the case of Ni this tendency is, however, not so clear because the capture zone of a crowdion for I_{61} is not so small as shown in Fig. 8, suggesting that even interstitial clusters have significant bias effect in Ni.

3.3 Interaction between a stacking fault tetrahedron (SFT) and point defects

Capture zones of SIAs and a vacancy were also obtained for a stacking fault tetrahedron in Ni. Stacking fault tetrahedron is one of the stable vacancy clusters in fcc metals and consists of six stair-rod dislocations and four stacking fault planes of a triangular shape. A stair-rod dislocation is an edge dislocation having a Burgers vector

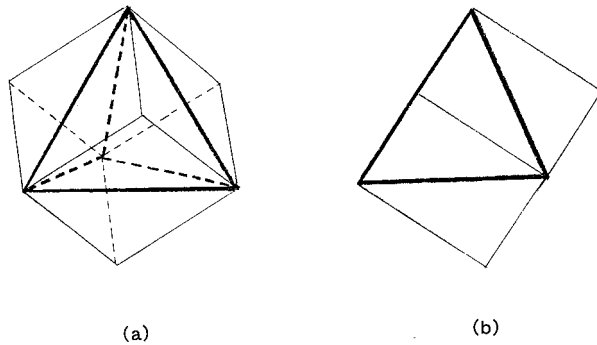


Figure 9 : A cube surrounded by six slip planes of six stair-rod dislocations belonging to a stacking fault tetrahedron in Ni viewed from two different directions (a) near $\langle 112 \rangle$ and (b) $\langle 110 \rangle$.

$a/6\langle 110 \rangle$, namely of the strength $b/3$ (one third of a perfect dislocation). Although this stair-rod dislocation is a sessile one, slip plane can be defined in a formal way, and six slip planes of six stair-rod dislocations form a cube as drawn in Fig. 9, where the cube is drawn viewed from two different directions (a) (near $\langle 112 \rangle$) and (b) ($\langle 110 \rangle$). Since a stair-rod dislocation (edge dislocation) has a compressive strain field above the slip plane and a tensile strain field below the slip plane, the interior of the cube is basically a region of tension and the outside of the cube is a region of compression. This basic aspect suggests that an SFT has a capture zone for an SIA inside the cube in Fig. 9, and has a capture zone for a vacancy outside of it. In Ni model crystal an SFT of 28 vacancies was constructed and the behavior of the interaction between this SFT and SIAs or a vacancy was studied. In Fig. 10 capture zone is shown for a crowdion around a SFT V_{28} in Ni observed on $\{110\}$ and $\{100\}$ planes (hatched planes in the figure). In Fig. 11 the same result is shown for a dumbbell around an SFT V_{28} in Ni observed on $\{110\}$ and $\{100\}$ planes (hatched planes in the figure). In both Figs. 10 and 11 capture zones have a rectangular shape on the $\{110\}$ plane and have a square shape on the $\{100\}$ plane, consistent with the cross section of the cube shown in Fig. 9. The actual size of the calculated capture zone for SIAs is larger than the cross section of the cube. We speculate that an SIA, especially a crowdion easily moves toward a stable position during relaxation, giving rise to a larger capture zone than that expected in Fig. 9. In Fig. 12 the capture zone is shown for a vacancy in Ni observed on $\{110\}$ and $\{100\}$

Ni
Interaction between SFT(V_{28}) and
a Crowdion

(Contour of -0.067 eV (500°C))

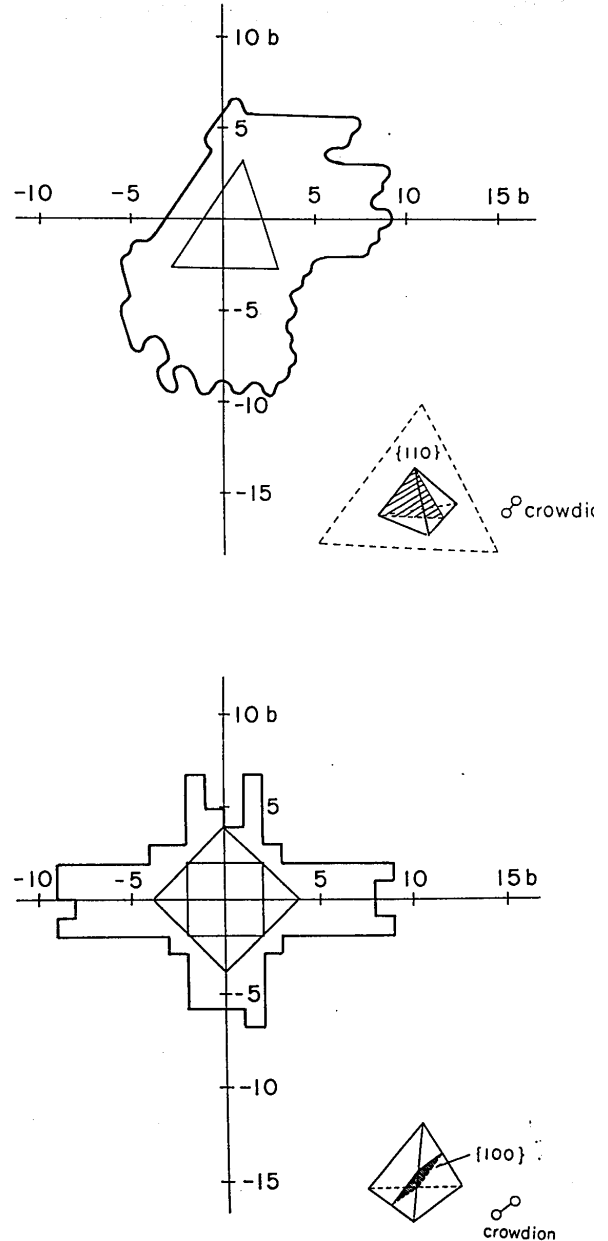


Figure 10 : The calculated capture zone for a crowdion around an SFT V_{28} in Ni observed on $\{110\}$ and $\{100\}$ planes (hatched planes in the figure).

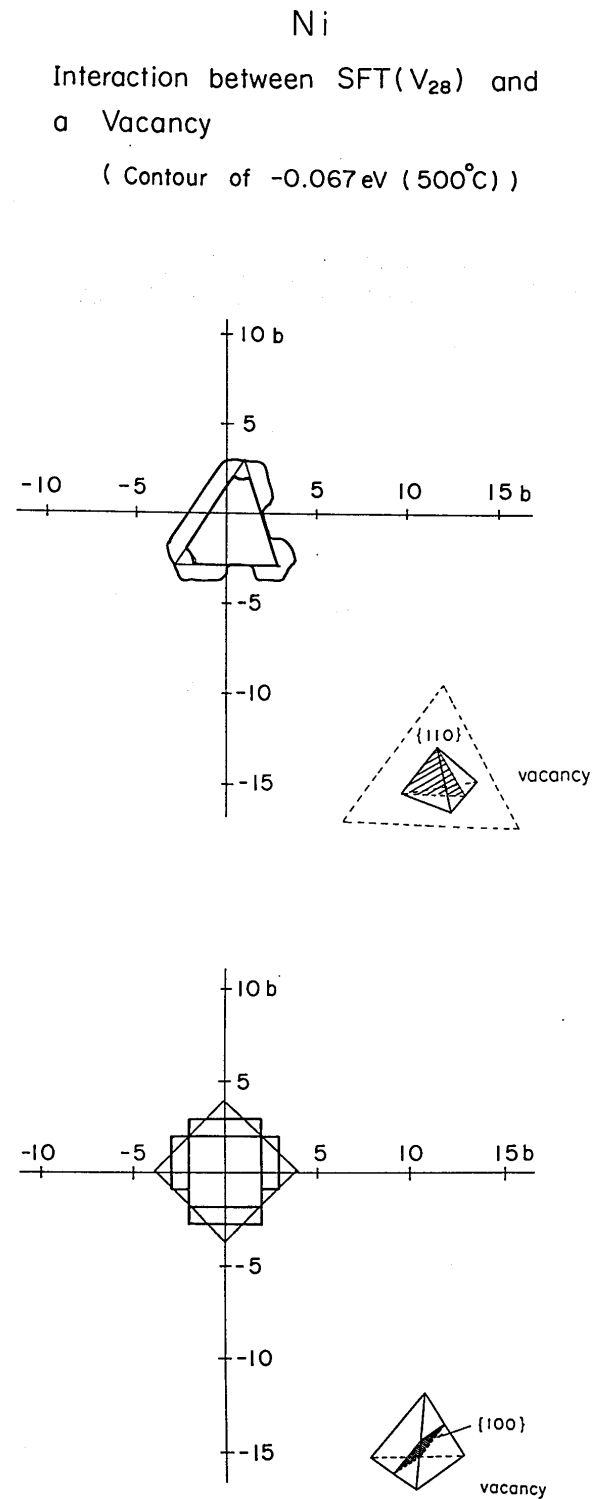
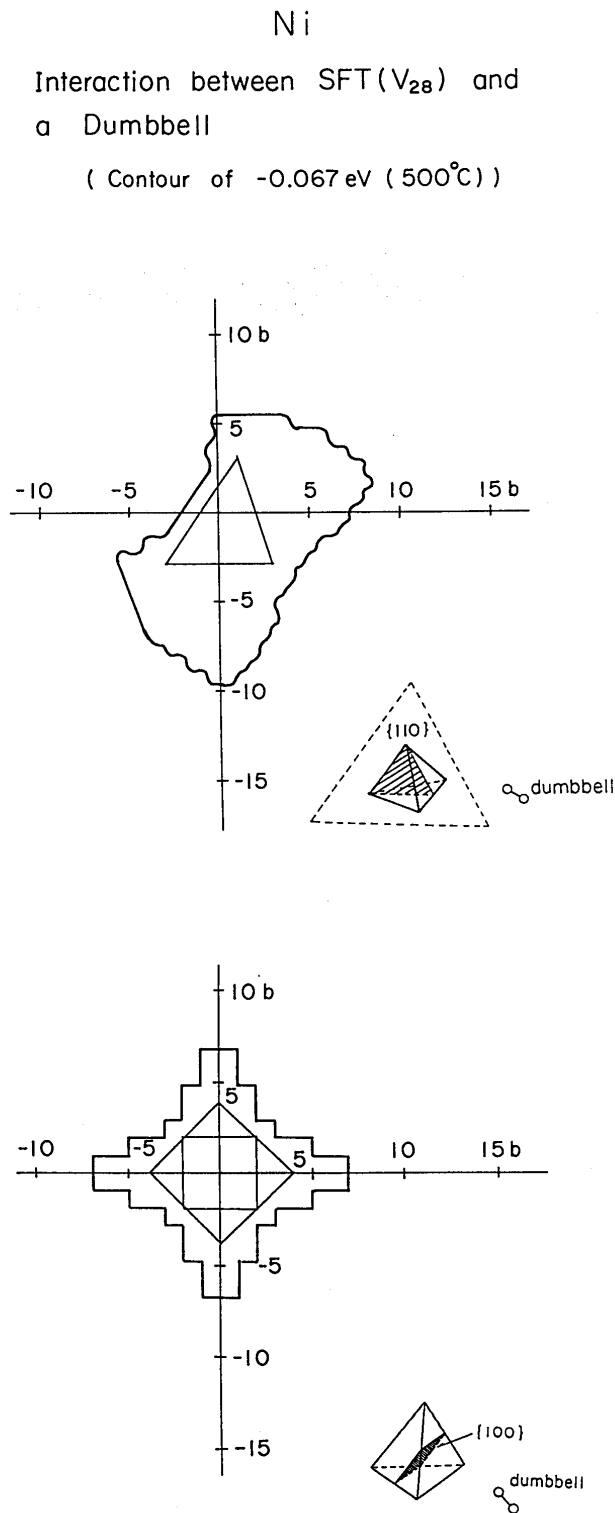


Figure 11 : The calculated capture zone for a dumbbell around an SFT V_{28} in Ni observed on $\{110\}$ and $\{100\}$ planes (hatched planes in the figure).

Figure 12 : The calculated capture zone for a vacancy around an SFT V_{28} in Ni observed on $\{110\}$ and $\{100\}$ planes (hatched planes in the figure).

planes (hatched planes in the figure), where a vacancy is trapped at a narrow region outside the cube. Anyway capture zones for SIAs to an SFT V_{28} seem larger than that for a vacancy in Ni. More detailed information, e.g., dependence of the capture zone on the size of SFTs, whose number is not magic, i.e, SFTs with steps need to be studied in the near future.

4 Conclusion

Calculated capture zones for $T = 500^\circ\text{C}$ for SIAs (crowdion and dumbbell) around a straight edge dislocation is larger than that for a vacancy in both Fe and Ni. Capture zones for Ni are larger than those for Fe, suggesting that Ni (fcc) has a larger dislocation bias factor than Fe (bcc). The capture zone calculated for an interstitial cluster (dislocation loop) I_{61} is smaller than that for a straight edge dislocation, especially in Fe. Capture zones were also calculated for an SFT V_{28} in Ni, indicating a larger capture zone for SIAs (crowdion and dumbbell) and a smaller capture zone for a vacancy.

References

- R. Bullough, B. L. Eyre and K. Krishan**, Proc. Roy. Soc. London A346 (1975) 81.
- C. H. Woo and B. N. Singh**, Phil. Mag. A65 (1992) 889.
- T. Diaz de la Rubia and M. W. Guinan**, Phys. Rev. Lett. 66 (1991) 2766.
- N. Soneda and T. Diaz de la Rubia**, Phil. Mag. A78 (1998) 995.
- M. W. Finnis and J. E. Sinclair**, Phil. Mag. A50 (1984) 45, (erratum: Phil. Mag. A53 (1986) 161).
- F. Gao, D. J. Bacon and G. J. Ackland**, Phil. Mag. A67 (1993) 275.
- E. Kuramoto**, J. Nucl. Mat., 276 (2000) 143.
- E. Kuramoto, K. Ohsawa and T. Tsutsumi**, J. Nucl. Mat. 271& 272 (1999) 26.
- M. Koyanagi, K. Ohsawa and E. Kuramoto**, J. Nucl. Mat. 271& 272 (1999) 205.
- W. G. Wolfer**, J. Phys. F: Met. Phys., 12 (1982) 425.
- V. V. Kirsanov and T. E. Turkebaev**, J. Nucl. Mat. 140 (1986) 264.
- H. Kamiyama, H. Rafii-Tabar, Y. Kawazoe and H. Matsui**, J. Nucl. Mat. 212-215 (1994) 231.